



FIREHOLE
TECHNOLOGIES
ADVANCED COMPOSITES ANALYSIS

VALIDATION OF HELIUS:MCT™ SIMULATIONS VERSUS EXPERIMENTS

Results for the First World-Wide Failure Exercise

Firehole Technologies Inc.

3/29/2010

VALIDATION OF HELIUS:MCT™ SIMULATIONS VERSUS EXPERIMENTS

Results for the First World-Wide Failure Exercise

Contents

Background.....	2
Comparison with Other Failure Technologies	2
WWFE-1 Case#1 - $\sigma_y:\sigma_{xy}$ failure of 0° E-Glass Epoxy Lamina	3
WWFE-1 Case#2 - $\sigma_y:\sigma_{xy}$ failure of 0° Carbon/Epoxy Lamina	4
WWFE-1 Case#3 - $\sigma_x:\sigma_y$ failure of 0° E-Glass/Epoxy Lamina.....	5
WWFE-1 Case#4- $\sigma_x:\sigma_y$ failure of [90°/±30°] E-Glass/Epoxy Laminate	6
WWFE-1 Case#5- $\sigma_x:\sigma_{xy}$ failure of [90°/±30°] E-Glass/Epoxy Laminate	7
WWFE-1 Case#6 - $\sigma_x:\sigma_y$ failure of [0°/±45°/90°] _S Carbon/Epoxy laminate.....	8
WWFE-1 Case#7 - Stress-Strain response of [0°/±45°/90°] _S Carbon/Epoxy laminate under uniaxial tension	9
WWFE-1 Case#8 - Stress-Strain response of [0°/±45°/90°] _S Carbon/Epoxy laminate under $\sigma_y:\sigma_x = 2:1$ biaxial Loading	10
WWFE-1 Case#9 - $\sigma_y:\sigma_y$ failure of [±55°] _S E-Glass/Epoxy laminate	11
WWFE-1 Case#10- Stress-Strain response of [±55°] _S E-Glass/Epoxy laminate under uniaxial tension	13
WWFE-1 Case#11- Stress-Strain response of [[±55°] _S E-Glass/Epoxy laminate under $\sigma_y:\sigma_x = 2:1$ biaxial Loading	14
WWFE-1 Case#12 stress-strain response of [0°/90°/0°] E-Glass/Epoxy laminate under uniaxial tension	15
WWFE-1 Case#13- Stress-Strain response of [±45°] _S E-Glass/Epoxy laminate under uniaxial tension	16
WWFE-1 Case#14- Stress-Strain response of [±45°] _S E-Glass/Epoxy laminate under $\sigma_y:\sigma_x = 1:-1$ biaxial loading	17
DISCUSSION	17
ACKNOWLEDGEMENTS.....	18
REFERENCES	18

BACKGROUND

The First World-Wide Failure Exercise (WWFE-1), circa 1998-2004, was a comprehensive effort aimed at evaluating numerous theories developed for predicting failure of high performance composite laminates under multiaxial loads (See Soden et al., 1998, 2002, Hinton et al., 2004, Kaddour et al., 2004). The Exercise required participants to make blind predictions for 14 different load cases that included four different material combinations involving glass/epoxy or carbon/epoxy continuous fiber laminates.

This document presents the results of Helius:MCT™ simulations of the 14 WWFE-1 test cases in comparison with the experimental results. In select cases, the results are also compared to “industry-standard” composite failure technologies.

Helius:MCT™ was developed to overcome the fundamental challenge encountered when addressing the problems like those posed in WWFE-1: efficiently crossing multiple geometric scales to capture the microstructural information where failure initiates while recognizing the practical constraints imposed by the size of the laminate (structure).

COMPARISON WITH OTHER FAILURE TECHNOLOGIES

As a means of comparison, this documents presents simulation results for other common composite failure technologies. The data listed as “Tsai-Wu” and “Hashin” was generated using Abaqus/Standard v 6.8 using the parameters or procedures listed in the Abaqus documentation. The data listed as “LaRC02” was produced using NEi NASTRAN version 9.2, again using all parameters and procedures recommended by the developers of the code (See Ragionieri and Weinberg 2006).

WWFE-1 CASE#1 - $\sigma_y:\sigma_{xy}$ FAILURE OF 0° E-GLASS EPOXY LAMINA

The Helius:MCT failure predictions for the biaxial, $\sigma_y:\sigma_{xy}$, failure envelope for a 0° E-Glass/LY556/HT907/DY063 lamina, shown in Figure 1, are in excellent agreement with the experimental data. This test case displays the a unique feature of Helius:MCT - strength enhancement in the presence of hydrostatic stresses.

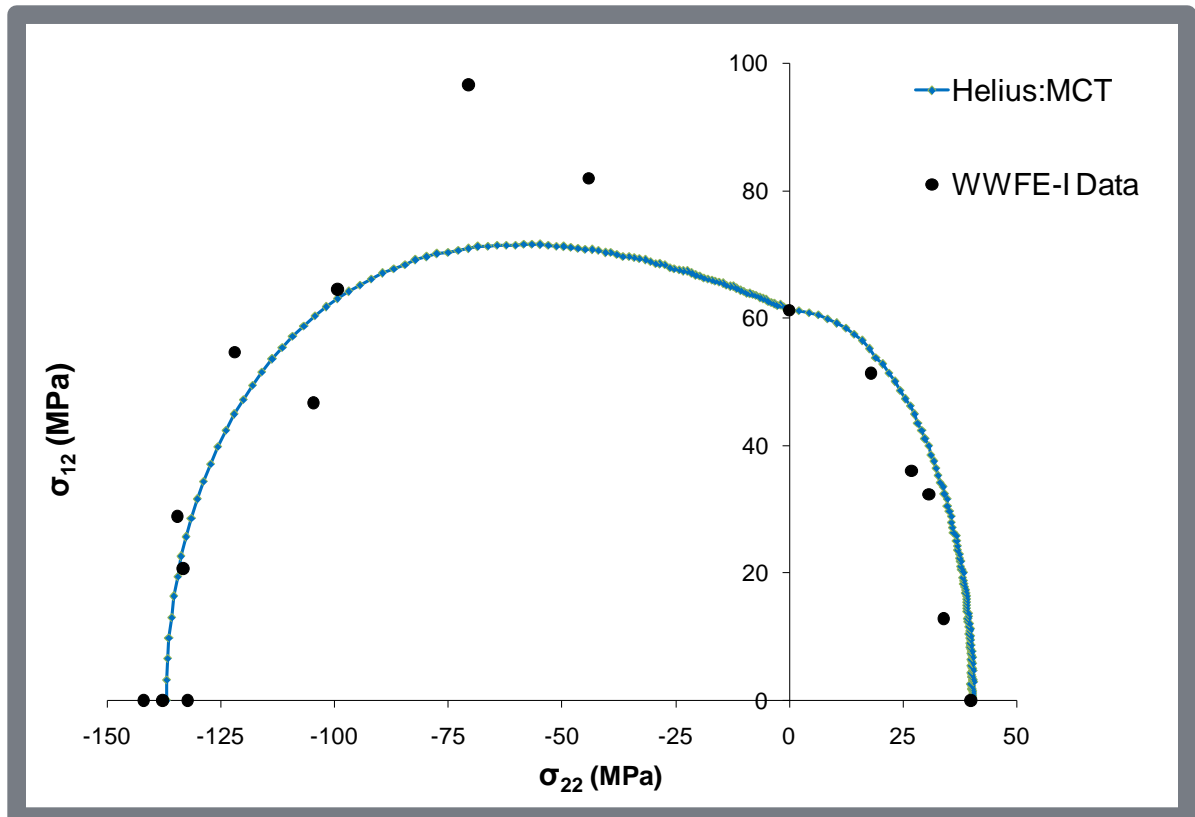


Figure 1

WWFE-1 CASE#2 - $\sigma_y:\sigma_{xy}$ FAILURE OF 0° CARBON/EPOXY LAMINA

The biaxial, $\sigma_x:\sigma_{xy}$, final failure envelope for a 0° lamina made of CFRP T300/914C material is shown in Figure 2. We note that unlike *Case 1*, there is no hydrostatic strength enhancement as the axial stress is in the fiber direction. Because the fibers carry so much of the load, the resulting hydrostatic stress in the matrix is relatively low.

An important point to note in the WWFE is that many of the failure envelopes provided represent the collective works of multiple investigators who may have used differing test methods, Soden (2004 b). Not surprisingly, such a data collection will produce large amounts of scatter for which no theory can accommodate. *Case 2* is an example of this phenomenon and we further this discussion in *Case 6*. The use of multiple data sets, while a necessity, forces one to temper quantitative arguments as to the correlation between theory and experiment. It should also be noted that the Hashin failure criterion performs nearly as well as the multi-scale approach of Helius:MCT. This is expected as the traditional failure technologies were developed for single-ply lamina.

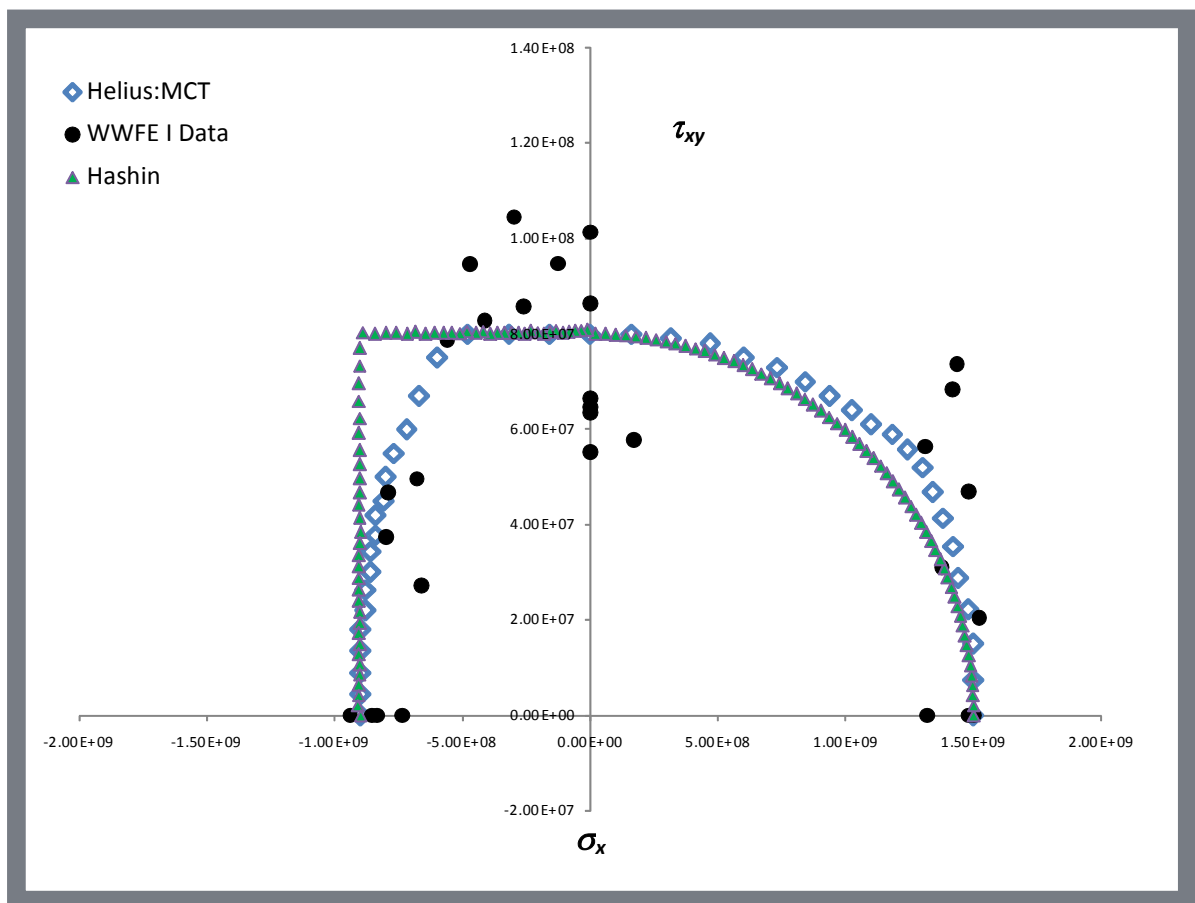


Figure 2

WWFE-1 CASE#3 - $\sigma_x:\sigma_y$ FAILURE OF 0° E-GLASS/EPOXY LAMINA

The failure envelope shown in Figure 3 is for a biaxial, $\sigma_x:\sigma_y$, loading of a 0° lamina of E-glass/MY750 epoxy. The excellent correlation with experiment in this case is due to the fact that Helius:MCT includes the effect of matrix stresses in the fiber direction, something not captured in homogenized approaches such as the Larc02 example displayed in Figure 3.

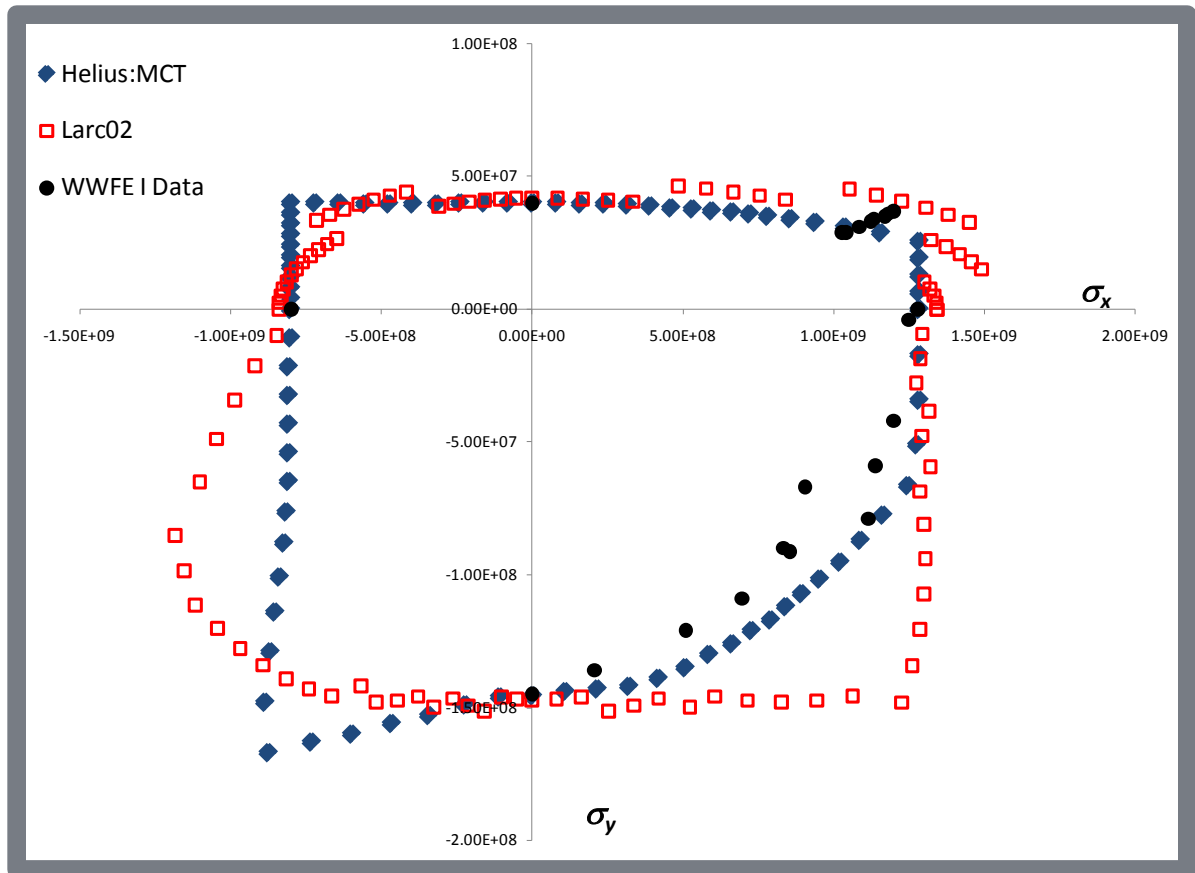


Figure 3

WWFE-1 CASE#4- $\sigma_x:\sigma_y$ FAILURE OF $[90^\circ/\pm 30^\circ]$ E-GLASS/EPOXY LAMINATE

The failure envelope shown in Figure 4 is for a biaxial, $\sigma_y:\sigma_x$ loading of a $[90^\circ/\pm 30^\circ]$ laminate made from E-glass/LY556/HT907/DY063. Helius:MCT results in quadrant I and IV are in good agreement with the experimental data and generally conservative. For a $\sigma_y:\sigma_x=1:1$ loading the Helius:MCT results are within 5% of the experimental failure whereas the Tsai-Wu criteria predicts failure 85% lower than shown in the experiment. The results in quadrants II and III are governed by buckling which was not considered in this analysis. The general conservatism of the Tsai-Wu predictions provide further evidence to the support the use of a multiscale progressive failure simulation technology.

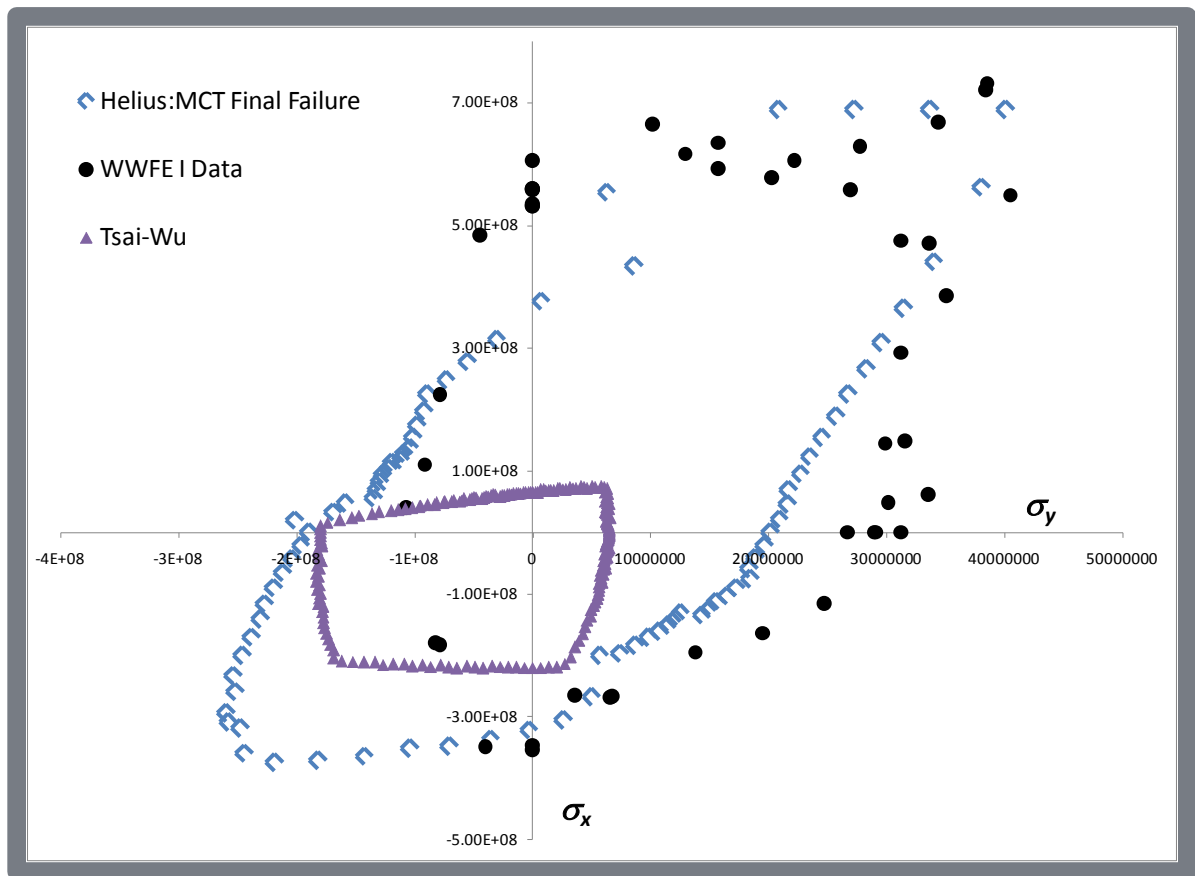


Figure 4

WWFE-1 CASE#5- $\sigma_x:\sigma_{xy}$ FAILURE OF $[90^\circ/\pm 30^\circ]$ E-GLASS/EPOXY LAMINATE

The failure envelope shown in Figure 5 is for a biaxial, $\sigma_x:\sigma_{xy}$, loading of a $[90^\circ/\pm 30^\circ]$ laminate made from E-glass/LY556/HT907/DY063. This case illustrates the extreme conservatism of analysis using a conventional Tsai-Wu first-ply-failure-approach. Along the $\sigma_x = 0$ axis, failure is predicted at approximately 1/10 of the experimental result using Tsai-Wu. The Helius:MCT result is also conservative, predicting failure approximately 60% of the measured value. Since the laminate contains no fibers spanning the x-axis, it is suspected that significant material nonlinearity in the matrix may exist in some loading scenarios, and the use of one the more sophisticated material models provided by Helius:MCT may capture behavior better.

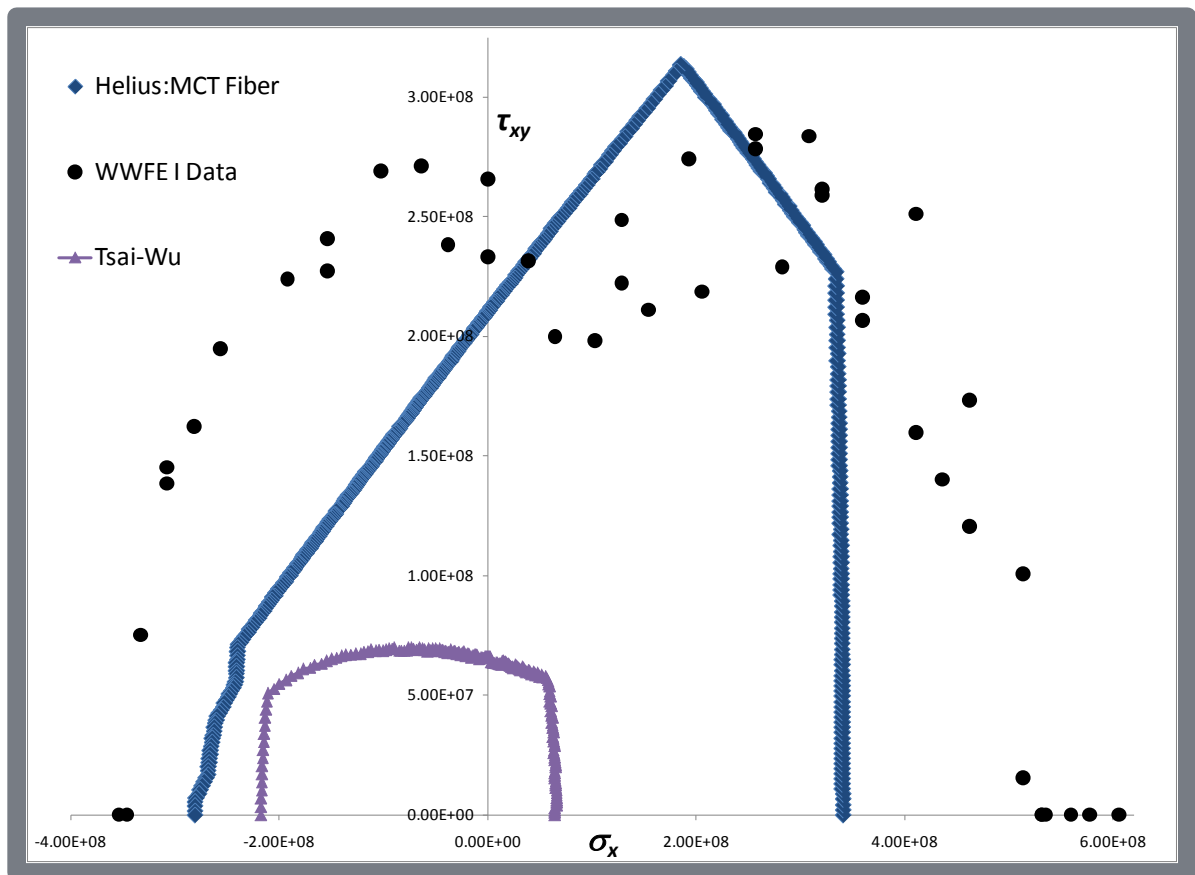


Figure 5

WWFE-1 CASE#6 - $\sigma_x:\sigma_y$ FAILURE OF $[0^\circ/\pm 45^\circ/90^\circ]_S$ CARBON/EPOXY LAMINATE

Figure 6 shows a complete failure envelope for the AS4/3501-6, $[0^\circ/\pm 45^\circ/90^\circ]_S$ laminate. The test case is considered important because this case represents a widely used material and laminate configuration. Excellent correlation is observed between the analytical and experimental $\sigma_x:\sigma_y$ failure envelopes in quadrant I and good correlation is seen in quadrant IV. The Tsai-Wu criterion results in this example show a significant amount of conservatism.

The results in quadrant IV are an example of the multiple data sets used to generate the WWFE experimental envelope. Specifically, note the inconsistency of the ultimate strengths along the compressive x (vertical) axis. Loading along this axis is dominated by the unidirectional compressive strength of the material in the fiber direction. A lowering of this unidirectional compressive strength, based on a different input strength, would produce an outstanding fit to the data in quadrant IV. In brief, this shows that Helius:MCT is capable of outstanding failure predictions, given a consistent set of data.

Finally, the lack of correlation in quadrant III, compression-compression loading, is likely due to buckling of the test specimen, as noted by Soden (2004 b), which is not accounted for in the Helius:MCT failure criteria.

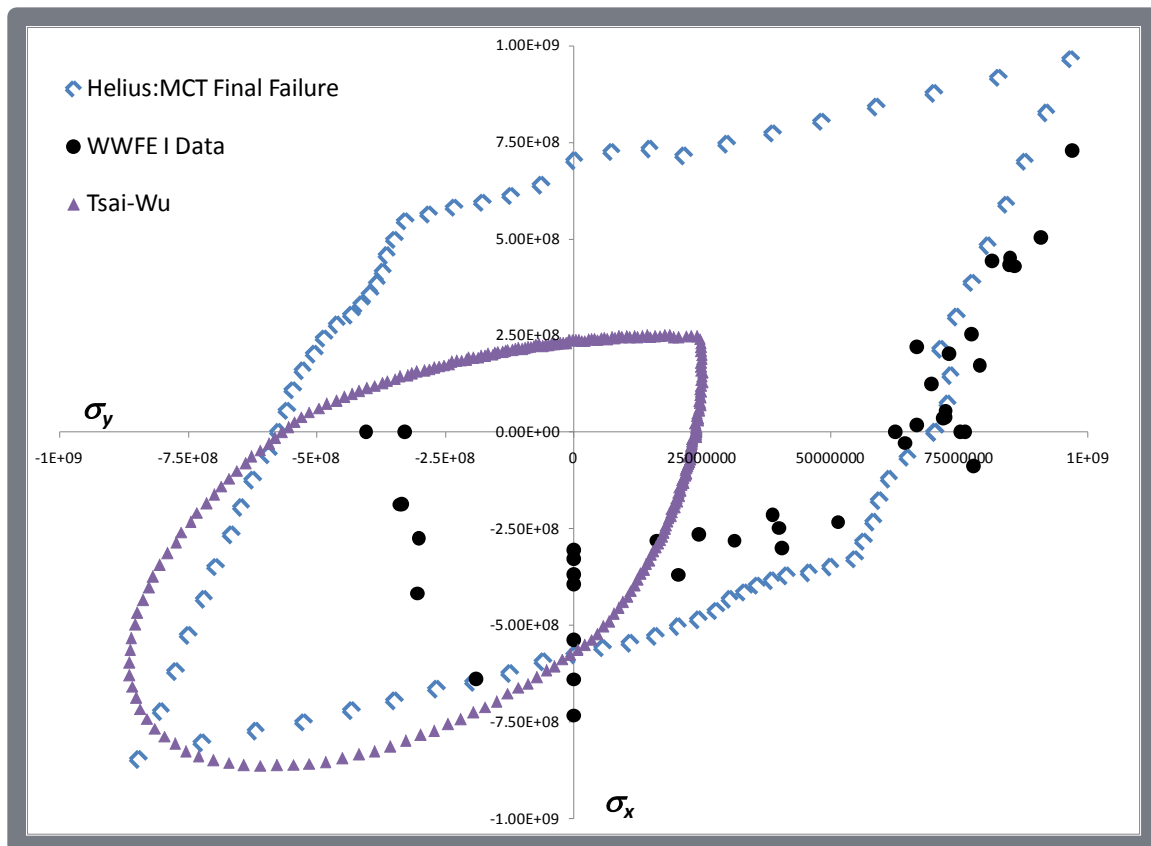


Figure 6

WWFE-1 CASE#7 - STRESS-STRAIN RESPONSE OF $[0^\circ/\pm 45^\circ/90^\circ]_S$ CARBON/EPOXY LAMINATE UNDER UNIAXIAL TENSION

The stress-strain curve for a AS4/3501-6, $[0^\circ/\pm 45^\circ/90^\circ]_S$ laminate under uniaxial tension, $\sigma_y:\sigma_x = 1:0$, is shown in Figure 7. Intermediate damage, predicted around 400 MPa in the form of matrix failure in the $\pm 45^\circ$ lamina, is caused by combined shear and tensile stresses. The organizers (Soden, 2004b) note that a decrease in the slope of the experimental stress-strain curve around 400 MPa indicated a form of initial failure in the actual laminate. The Helius:MCT analysis shows good results in the predicted response, even above above 400 MPa. This is a good example of the unique post-failure degradation feature of Helius:MCT. Note that the Helius:MCT ultimate failure predictions is within 1 % the ultimate laminate strength. The LaRC02 results show good initial correlation, but predict an ultimate failure at the point of initial matrix damage – under predicting the ultimate failure by nearly 200%.

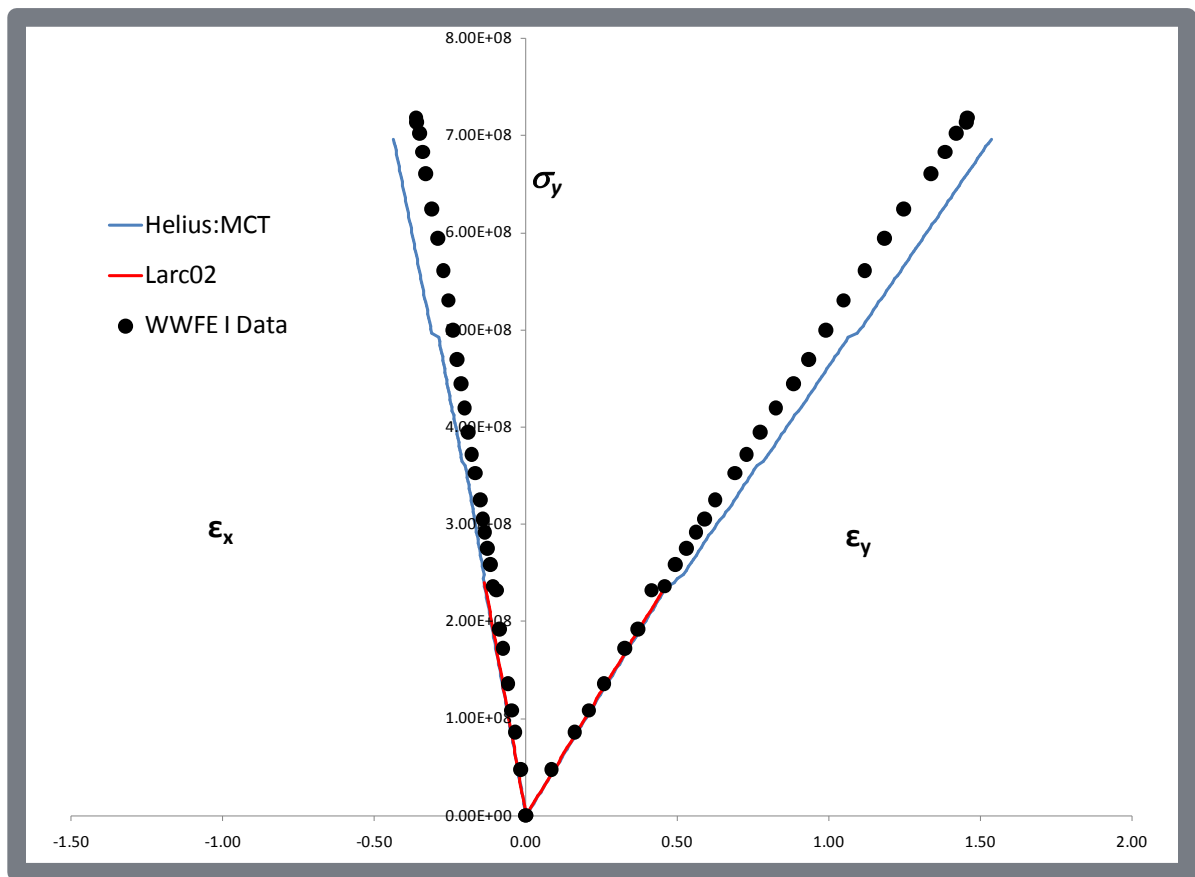


Figure 7

WWFE-1 CASE#8 - STRESS-STRAIN RESPONSE OF $[0^\circ/\pm 45^\circ/90^\circ]_S$ CARBON/EPOXY LAMINATE UNDER $\sigma_y:\sigma_x = 2:1$ BIAXIAL LOADING

The stress-strain response for the AS4/3501-6, $[0^\circ/\pm 45^\circ/90^\circ]_S$, laminate under $\sigma_y:\sigma_x = 2:1$ biaxial tension is shown in Figure 8. As in Case 7, the Helius:MCT results show good correlation both before and after the response becomes nonlinear due to localized matrix damage. Again, the homogenized approaches– in this case both the Tsai-Wu and LaRC02 criteria are shown– vastly under predict the actual failure.

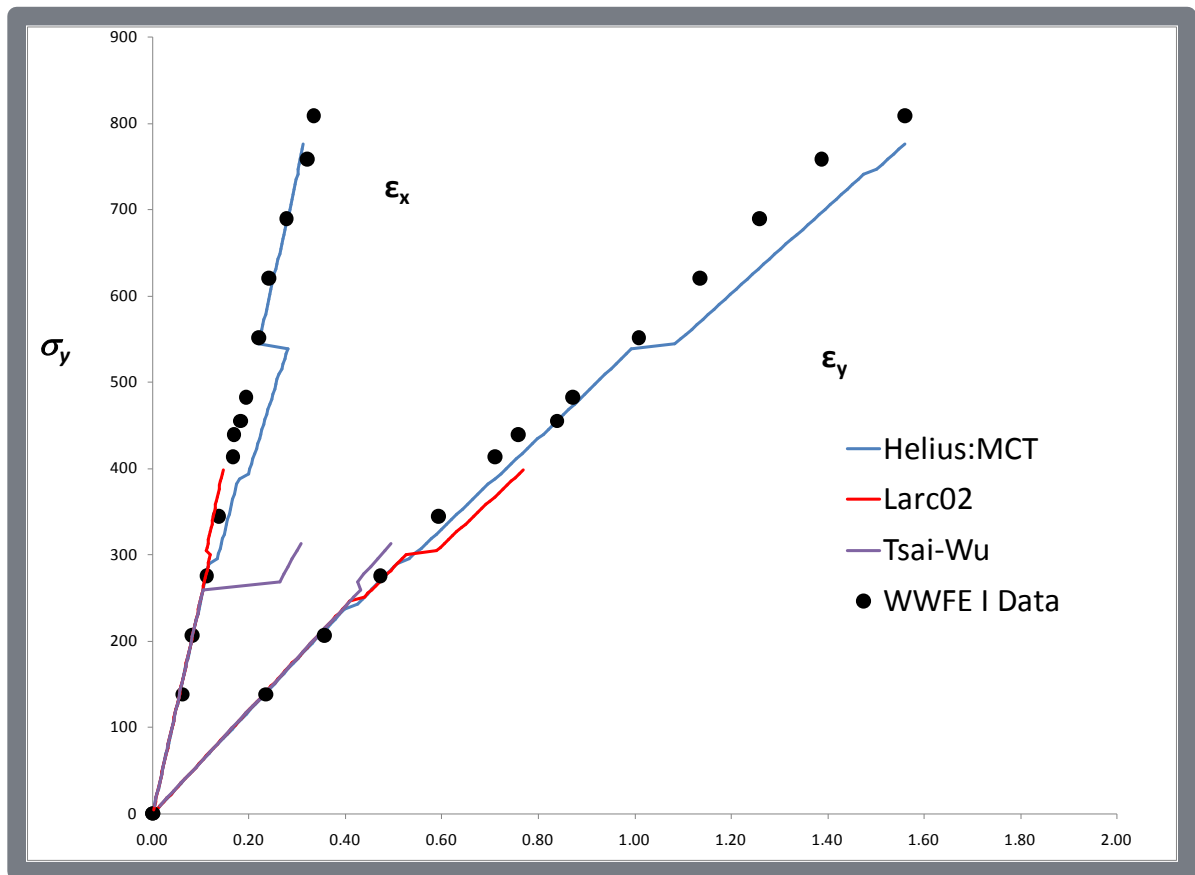


Figure 8

WWFE-1 CASE#9 - $\sigma_y:\sigma_x$ FAILURE OF $[\pm 55^\circ]_S$ E-GLASS/EPOXY LAMINATE

Figure 9 shows a complete failure envelope for $\sigma_y:\sigma_x$ loading of an E-glass/MY750/HY917/DY063 $[\pm 55^\circ]_S$ laminate. Helius:MCT results show good overall agreement with the test data for this highly complex failure envelope. In addition, the unique nature of the failure envelope provides for little data in quadrants II and IV and the analytical results support this.

It is believed the data of quadrant I is questionable in that the loading—particularly the loads with large axial stresses, σ_{yy} , produces significant shear strains resulting in finite strain effects in the form of fiber orientation changes. Any reorienting of fibers may dramatically increase strengths and ultimate failure may be driven by fiber rupture. Also, the experimental data shown in Figure 9 is an assembly of several tests on composite tubes and is described by Soden (2004b) and may not be accurately captured using a simple laminate analysis.

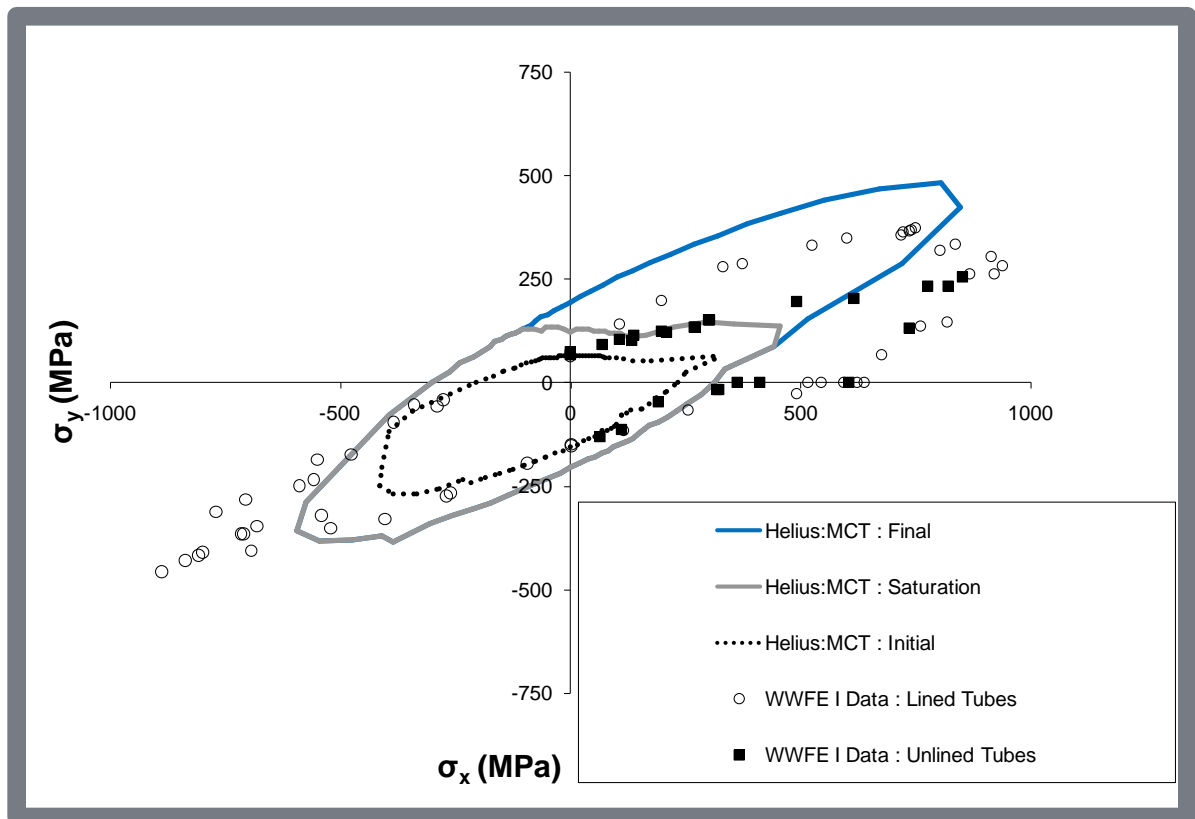


Figure 9

To illustrate the importance of identifying the role of each constituent in the final failure of the specimen, the data plotted in Figure 10 is limited to leakage through the wall of an unlined specimen. Leakage requires a continuous crack path that passes through each layer of the laminate. This scenario requires a dense network of matrix cracks in each layer of the laminate to increase the likelihood of continuous crack paths. In order to identify this

scenario, the Helius:MCT feature to model matrix crack saturation was used to model the scenario where matrix cracks exist in all plies in order for this significant leakage to take place.

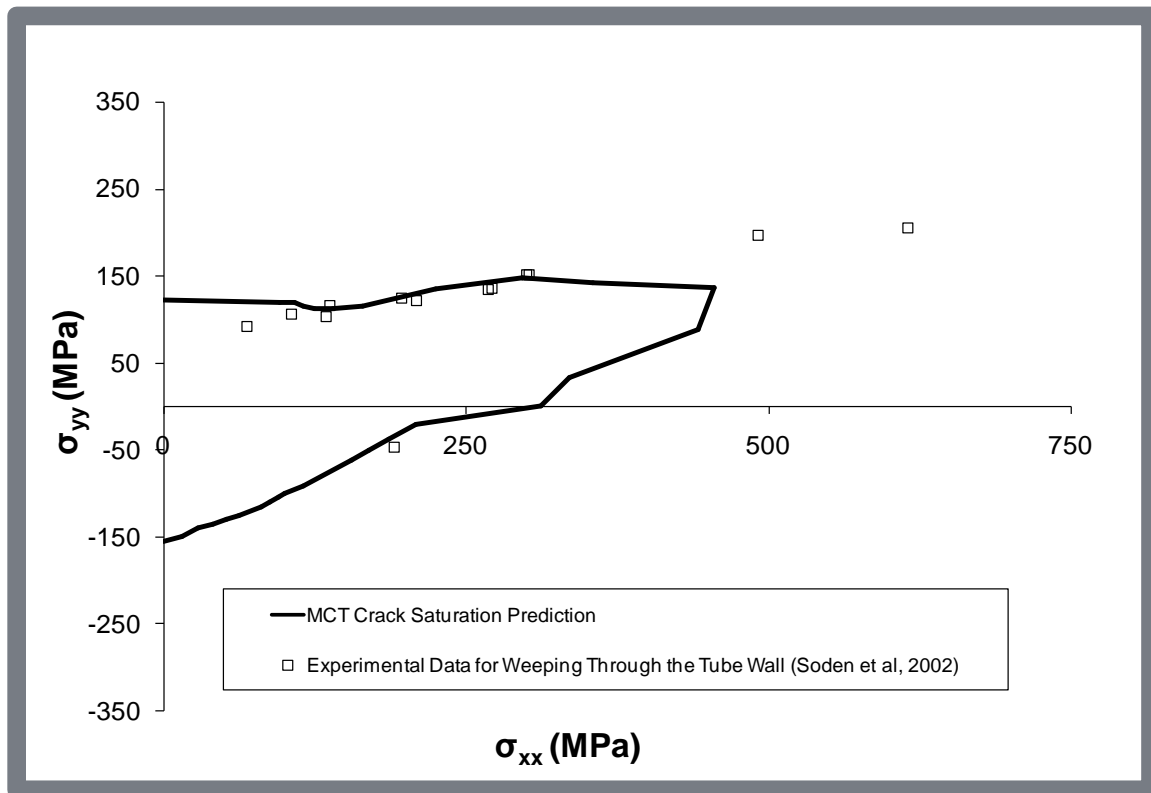


Figure 10

Helius:MCT predictions for matrix crack saturation are compared to the weeping data in Figure 10. There is excellent agreement with the experimental data. Now consider the results in Figure 9. For a value of $\sigma_x = 270$ MPa, σ_y at fiber failure is 2.5 times greater the σ_y for matrix saturation. This supports the philosophy that multiscale information is need to accurately capture the behavior of a composite structure as the definite of failure will change with service conditions.

WWFE-1 CASE#10- STRESS-STRAIN RESPONSE OF $[\pm 55^\circ]_S$ E-GLASS/EPOXY LAMINATE UNDER UNIAXIAL TENSION

Non-linear shear behavior characterizes the stress-strain curves of the E-glass/MY750/HY917/DY063, $[\pm 55^\circ]_S$ laminate under uniaxial load, $\sigma_y:\sigma_x = 1:0$, as shown in Figure 11. This case points out that, while Helius:MCT provides the analyst with significantly better results and more comprehensive information about the behavior of composites, engineering judgment of the analyst is still necessary. Specifically, the predictions of Helius:MCT are in good agreement with the experimental data up to about 250 MPa ($|\epsilon_x| = \epsilon_y = 2.0\%$) where we are declaring ultimate failure in shear through excessive deflection. In theory, the Helius:MCT analysis could continue to sustain load and further track the experimental data. However, note that finite strain effects causing angle changes in fiber orientations are occurring at strains beyond where we have terminated the analysis.

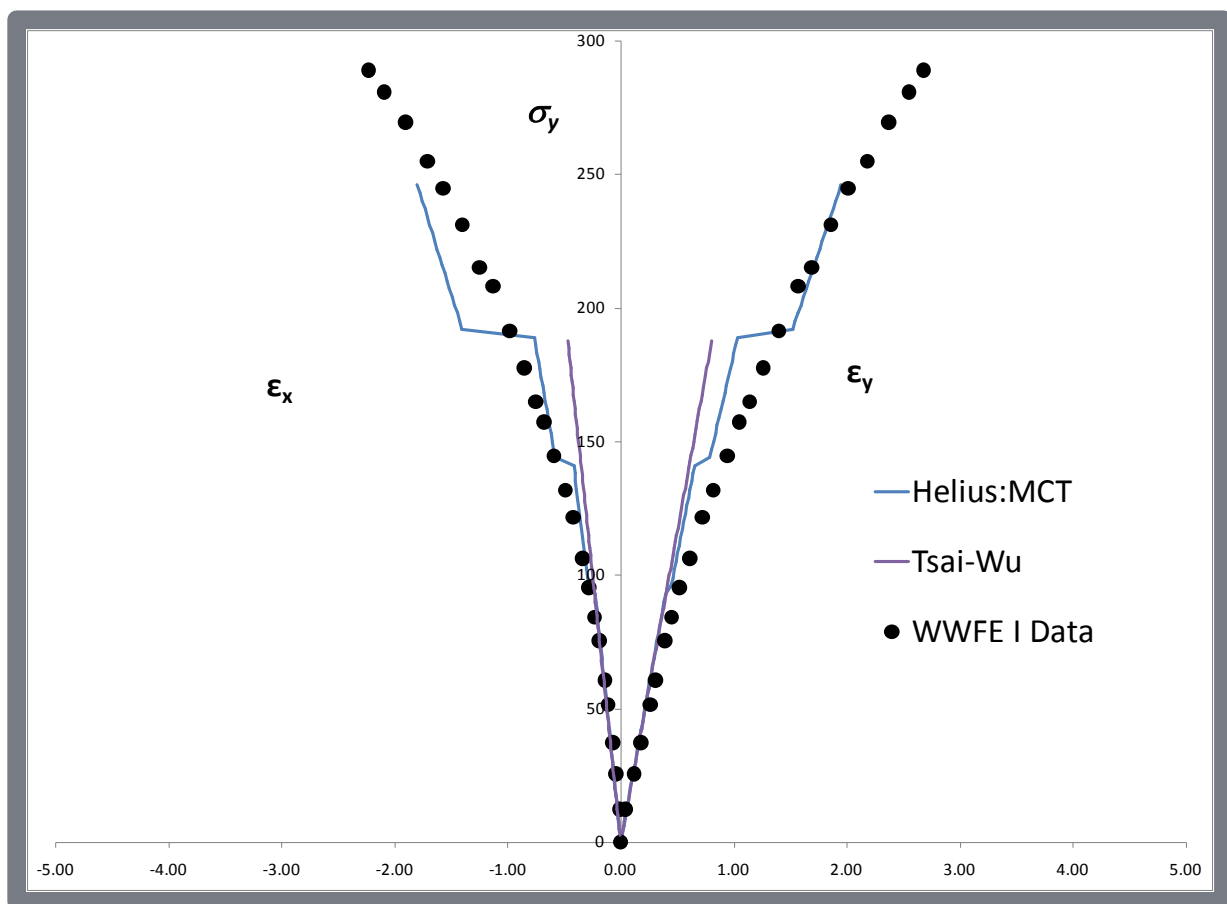


Figure 11

WWFE-1 CASE#11- STRESS-STRAIN RESPONSE OF $[[\pm 55^\circ]_S$ E-GLASS/EPOXY LAMINATE UNDER $\sigma_y:\sigma_x = 2:1$ BIAXIAL LOADING

Stress-strain data and predictions under $\sigma_y:\sigma_x = 2:1$ are shown in Figure 12 for the E-glass/MY750/HY917/DY063 $[\pm 55^\circ]_S$ laminate corresponding to *Case 9*. We are reluctant to draw any conclusions at all about the lack of correlation between theory and experiment due to the questionable nature of the data as discussed in *Case 9*. However, we note that the specific load path provided is susceptible to producing finite deformation effects resulting in fiber angle changes.

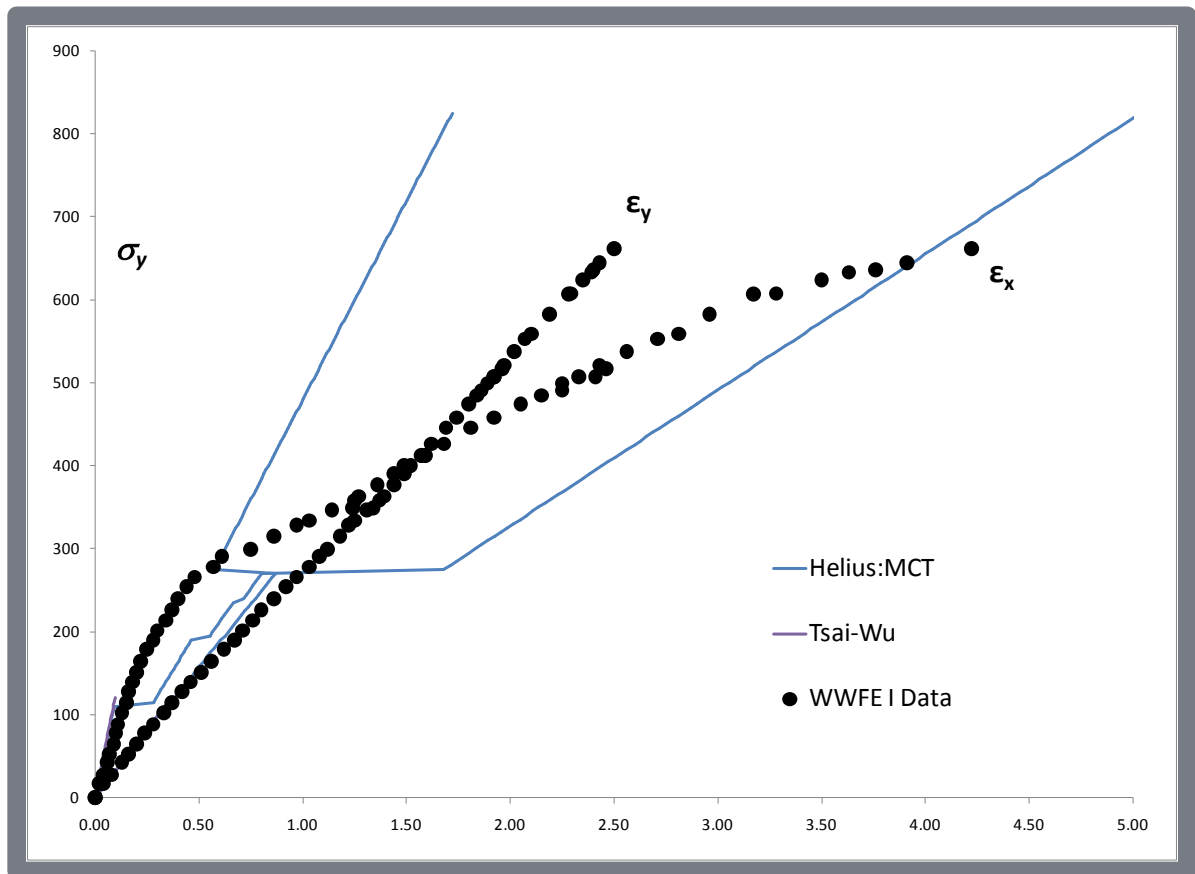


Figure 12

WWFE-1 CASE#12 STRESS-STRAIN RESPONSE OF $[0^\circ/90^\circ/0^\circ]$ E-GLASS/EPOXY LAMINATE UNDER UNIAXIAL TENSION

The E-glass/MY750/HY917/DY063 stress-strain curves for a $[0^\circ/90^\circ/0^\circ]$ laminate under uniaxial load, $\sigma_y:\sigma_x = 1:0$, are shown in Figure 12. Both versions of the MCT analysis perform remarkably well. The Helius:MCT ultimate laminate strength is predicted at 610 MPa, almost exactly at the experimental value of 609 MPa. Note that, again, the homogenized approaches such as the Larc02 are unable to capture any behavior beyond initial localized damage.

The good correlation in the case is an example of the material property degradation feature of Helius:MCT. The parameters used for degradation developed from Knops and Bögle (2006).

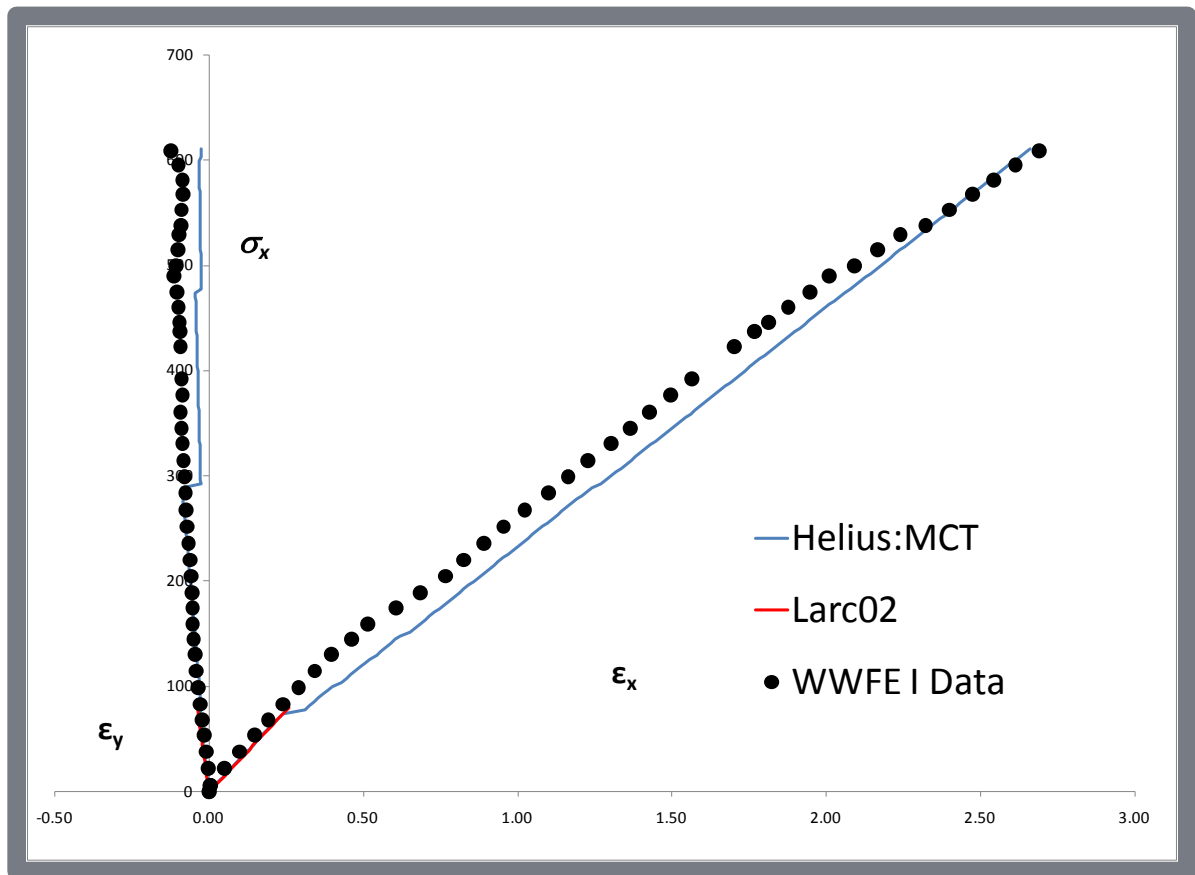


Figure 13

WWFE-1 CASE#13- STRESS-STRAIN RESPONSE OF $[\pm 45^\circ]_S$ E-GLASS/EPOXY LAMINATE UNDER UNIAXIAL TENSION

The test case shows stress-strain data for a E-glass/MY750/HY917/DY063, $[\pm 45^\circ]_S$ laminate under a biaxial load, $\sigma_y:\sigma_x = 1:1$. Again, Helius:MCT shows excellent correlation between the analytical and experimental stress-strain curves. Initial laminate damage due to tensile matrix failure in all lamina is predicted by at approximately 70 MPa which corresponds to the initial cracking noted by the organizers between 50-70 MPa. Crack saturation is predicted at 147 MPa, 32% below when leakage is reported through the wall of an unlined specimen. Final failure is predicted 26% higher than the experimental final failure.

The test specimens were reported to have a fiber volume fraction of 55% instead of the 60% given in the lamina data. This discrepancy could cause the under prediction of crack saturation and the over prediction of fiber failure.

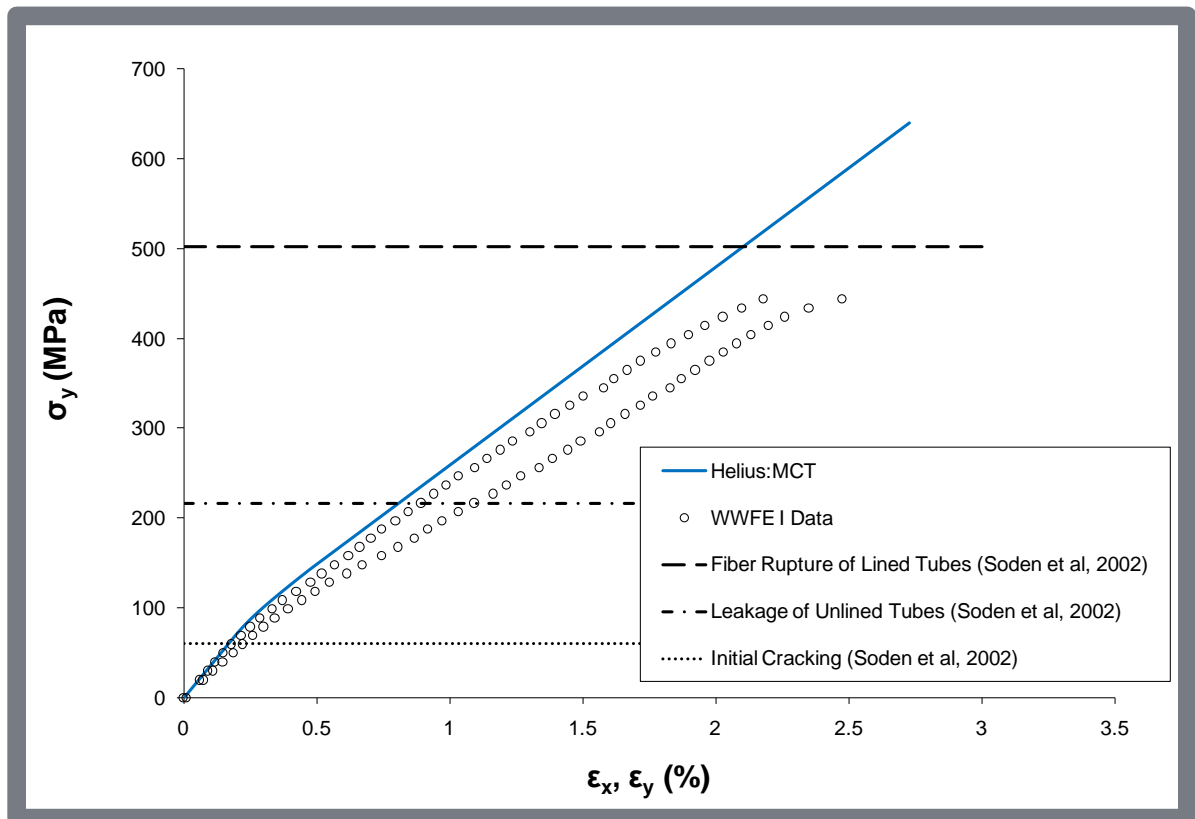


Figure 14

WWFE-1 CASE#14- STRESS-STRAIN RESPONSE OF $[\pm 45^\circ]_S$ E-GLASS/EPOXY LAMINATE UNDER $\sigma_y:\sigma_x = 1:-1$ BIAXIAL LOADING

Stress-strain curves for an E-glass/MY750/HY917/DY063, $[\pm 45^\circ]_S$ laminate under biaxial load, $\sigma_y:\sigma_x = 1:-1$, are shown in Figure 15. The lamina are in a state of pure shear in the local (material) coordinate system. Helius:MCT predictions are again in good agreement with the experimental data.

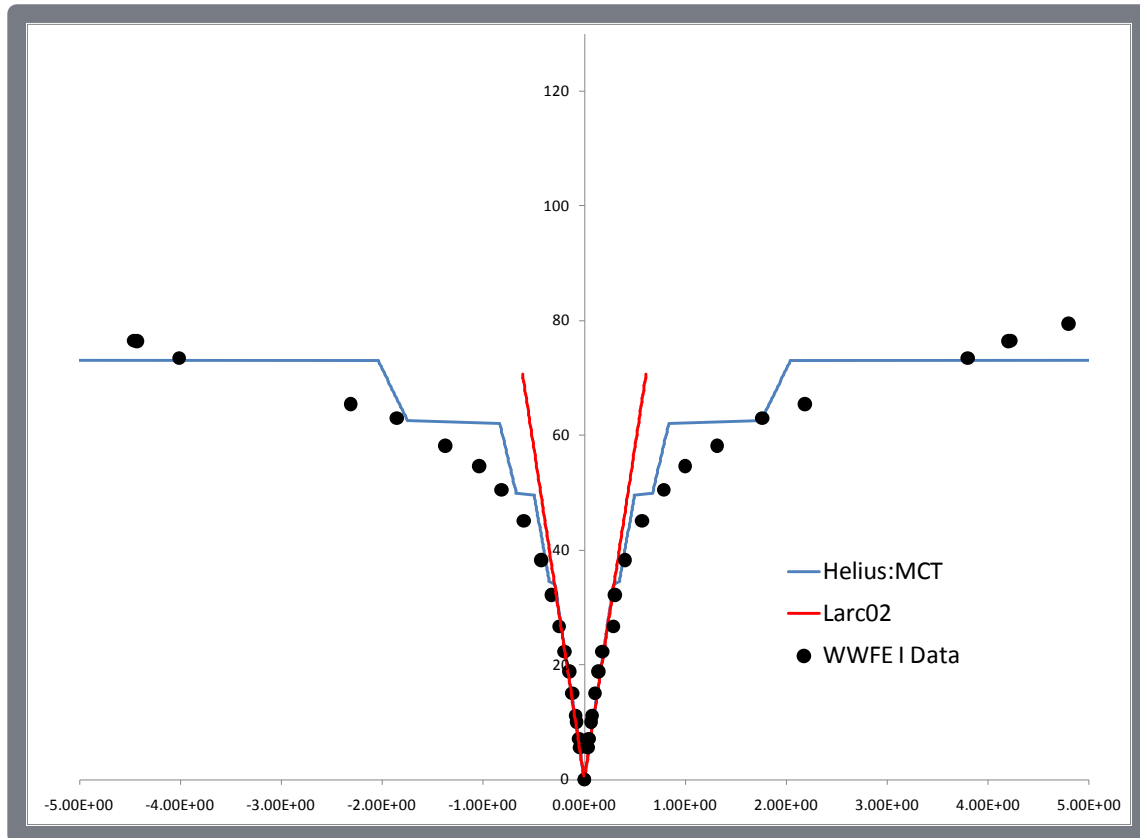


Figure 15

DISCUSSION

The Helius:MCT analysis presented here produced strong correlation with available experimental results from the first WWFE. An important feature of this analysis is that for carbon/epoxy composites, the parameters necessary to generate the analysis for any multidirectional laminate are attainable from a set of standard tests used to characterize a unidirectional composite material. These tests include longitudinal tension/compression, transverse tension/compression, transverse shear and longitudinal shear.

Ideally, in addition to the standard “uniaxial” tests one would also like to have biaxial $\sigma_{11}-\sigma_{22}$ of a unidirectional composite for glass/epoxy composites. In the absence of this data our experience suggests the anisotropic failure envelope of Hill (1950) provides an acceptable estimate of composite failure in quadrant IV. This failure point is the lone additional piece of information necessary to fully characterize glass/epoxy composites.

Finally, an important and distinguishing feature of Helius:MCT is the ease of use as these analyses were performed within a commercial finite element environment and the low computational burden of this multiscale approach. These features make Helius:MCT a suitable candidate for large scale nonlinear structural analysis (See additional Case Studies available from www.fireholetech.com) and distinguishes the approach for other multiscale methods that are often numerically untenable.

ACKNOWLEDGEMENTS

Firehole Technologies would like to acknowledge the Air Force Research Laboratory (AFRL) – Space Vehicles Directorate for their continued dedication to advancing the science of composite simulation.

REFERENCES

- Hashin, Z (1980), “Failure criteria for unidirectional fiber composites,” *Journal of Applied Mechanics*, Vol. 47, 329-334.
- Hill, R. (1950), *The Mathematical Theory of Plasticity*, Oxford University Press, London, England.
- Hill, R (1963), “Elastic properties of reinforced solids: Some theoretical principles,” *Jour. Mechanics and Physics of Solids*, Vol. 11, 357-372.
- Hinton, MJ, Kaddour, AS and PD Soden (2004), "The World-Wide Failure Exercise: Its origin, concept and content," *Failure Criteria in Fibre Reinforced Polymer Composites: The World-Wide Failure Exercise*, Eds. MJ Hinton, AS Kaddour and PD Soden, Elsevier, Kidlington, Oxford, UK, 2-26.
- Kaddour, AS, MJ Hinton, and PD Soden (2004), "Predictive capabilities of nineteen failure theories and design methodologies for polymer composite laminates. Part B: Comparison with Experiments," *Failure Criteria in Fibre Reinforced Polymer Composites: The World-Wide Failure Exercise*, Eds. MJ Hinton, AS Kaddour and PD Soden, Elsevier, Kidlington, Oxford, UK, 1073-1221.
- Knops, M and C Bögle (2006), “Gradual failure in fibre/polymer laminates” *Composite Science and Technology*, Vol. 66, 616-625.
- Ragionieri, S. and Weinberg D (2006). Finite Element Implementation of Advanced Failure Criteria For Composites. Noran Engineering Inc. White paper.
- Soden PD, MJ Hinton, and AS Kaddour (1998), “Lamina properties, lay-up configurations and loading conditions for a range of fibre-reinforced composite laminates,” *Composites Science and Technology*, Vol. 58, 1011-1022.
- Soden PD, MJ Hinton, and AS Kaddour (2002), “Biaxial test results for strength and deformation of a range of e-glass and carbon fibre reinforced composite laminates: failure exercise benchmark data,” *Composites Science and Technology*, Vol. 62, 1489-1514.